Pulse shaping fiber laser at 1.5 μm

Peng Wan,[1,*] Jian Liu,[1] Lih-Mei Yang,[1] and Farzin Amzajerdian[2]

[1]PolarOnyx Inc., 2526 Qume Drive, Suites 17 & 18, San Jose, California 95131, USA

[2]NASA Langley Research Center, Mississippi 468, Hampton, Virginia 23681, USA

*Corresponding author: pwan@polaronyx.com

In this paper we present, for the first time to our knowledge, a new pulse shaping technology (modulation schemes for seed laser) used to mitigate pulse narowing effect and SBS effect in a high energy Er:Yb codoped fiber master oscillator power amplifier system at 1.5 μm to obtain longer pulse duration and higher energy. An average power of over 1.3 W and a pulse energy of over 0.13 mJ were obtained at 10 kHz repetition rate with a pulse duration of 200 ns and near-diffraction-limited beam quality ($M^2 < 1.2$). © 2012 Optical Society of America

OCIS codes: 060.3510, 140.0140, 140.3538, 140.4480.

1. Introduction

Fiber lasers are playing an increasingly important role in laser applications. All-fiber-based pulsed fiber lasers are particularly promising for laser sensing, velocimetry, laser imagery coherent Lidar, and free space communications due to its high efficiency, compact size, reliable operation, the ease of alignment, and the possibility of autonomous operation [1–7]. Various types of high power and high energy fiber lasers have been developed. Narrow linewidth outputs with 126 μJ [8], 200 μJ [9], and 290 μJ [10] from all-fiber based master oscillator power amplifiers (MOPAs) have been demonstrated.

In coherent optical sensing and lidar applications, high precision measurements demand long pulse duration and good pulse shape, as well as narrow linewidth. In the case of amplification of long duration narrow linewidth signals (<1 MHz) in fiber amplifiers, stimulated Brillouin scattering (SBS) induces strong limitation for achieving high peak powers in optical fibers. In addition, gain narrowing effect in high power fiber amplifiers can also deform the output pulse shape and shorten the pulse duration.

Recently, we have applied modulated pulse shape of seed laser to mitigate both SBS and gain narrowing effects in 1.5 μm fiber power amplifier. A fiber laser with 1.3 W average power and 0.13 mJ pulse energy output at a wavelength of 1.5 μm with pulse width of 200 ns were obtained. In this article, we will firstly introduce the experimental setup and pulse shaping method. Then SBS and gain narrowing effects are shown to be greatly reduced by using this method.

2. Experimental Setup

Figure 1 shows a schematic diagram of the laser system. The seed laser was a distributed-feedback (DFB) laser with 200 kHz linewidth. The central wavelength was around 1550 nm. The seed laser was driven by a laser diode driving board manufactured in house. The shaped pulse was generated by changing the driving current format of the directly-modulated DFB laser. The repetition rate was tuned from 10 kHz to 250 kHz and the pulse width was tuned from 10 ns to 4 μs in this experiment. The shaped pulses were sent to a two-stage preamplifier (A1 and A2). The preamplifiers were standard single mode erbium-doped fiber amplifiers, which had been optimized and characterized to provide an overall gain of 21.9 dB. Two 7 W multimode laser diodes were used as pumps for the final power amplifier
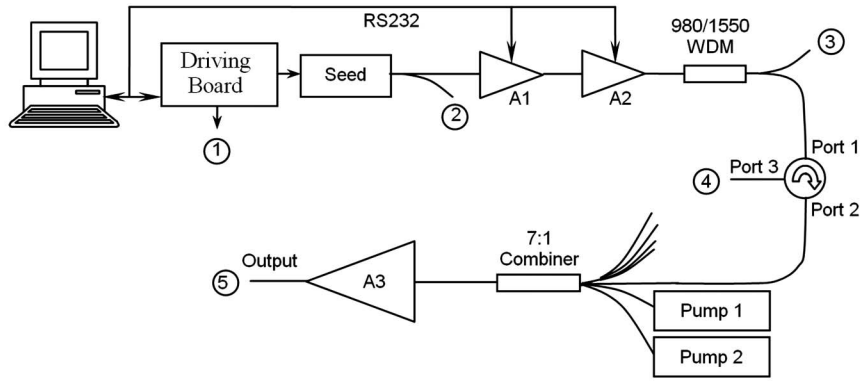
Fig. 1. Experiment system block diagram. There are five ports to monitor system and collect data. ① Electronic modulation signal from laser diode driving board; ② Seed laser monitor; ③ WDM monitor; ④ Circulator Port three to monitor back-reflected SBS; ⑤ Final output.

(A3). The active medium in the final amplifier was a commercial double-clad Er:Yb codoped fiber with a core diameter of 17 μm and a clad diameter of 200 μm.

3. Stimulated Brillouin Scattering and Pulse Narrowing

Nonlinear effects such as the optical Kerr effect, stimulated Raman scattering, and SBS have been observed in fiber amplifiers. In the case of amplifying narrow linewidth signal, the dominant nonlinear effect is SBS, which induces strong limitation for achieving high peak power in optical fibers. SBS arises from the interaction between optical field and acoustic phonons in the fiber [11–13]. Although the nonlinearity of silica is not very high, the high optical intensity and long propagation length inside the fiber can still result in strong nonlinear effects. At a high enough input power, SBS will convert transmitted light in the fiber to a scattered, Stokes-shifted reflection.

In a single mode optical fiber, the Brillouin frequency shift is given by

$$\nu_B = 2nV_a/\lambda, \tag{1}$$

where V_a is the speed of sound in the medium, n is the refractive index, and λ is the wavelength. If we choose $V_a = 5460$ m/s, $n = 1.5$ for glass, then we obtain the typical value of a Brillouin frequency shift in optical fiber at 1.5 μm of 10.5 GHz (corresponding to 0.084 nm shift in wavelength).
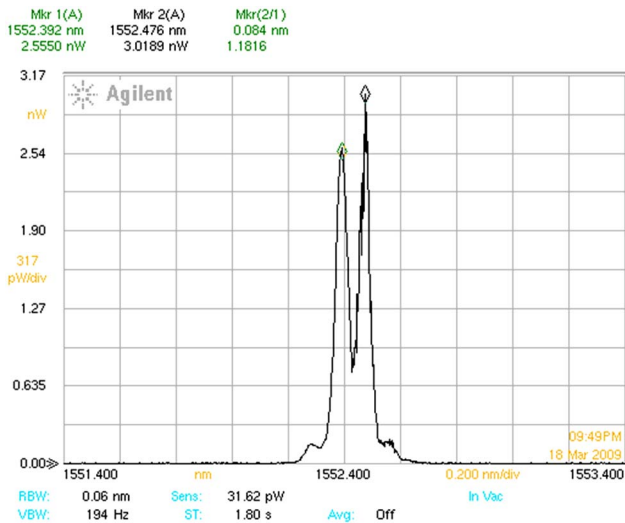

Fig. 2. (Color online) OSA spectrum of the SBS signal. A 0.08 nm wavelength shift can be seen clearly.
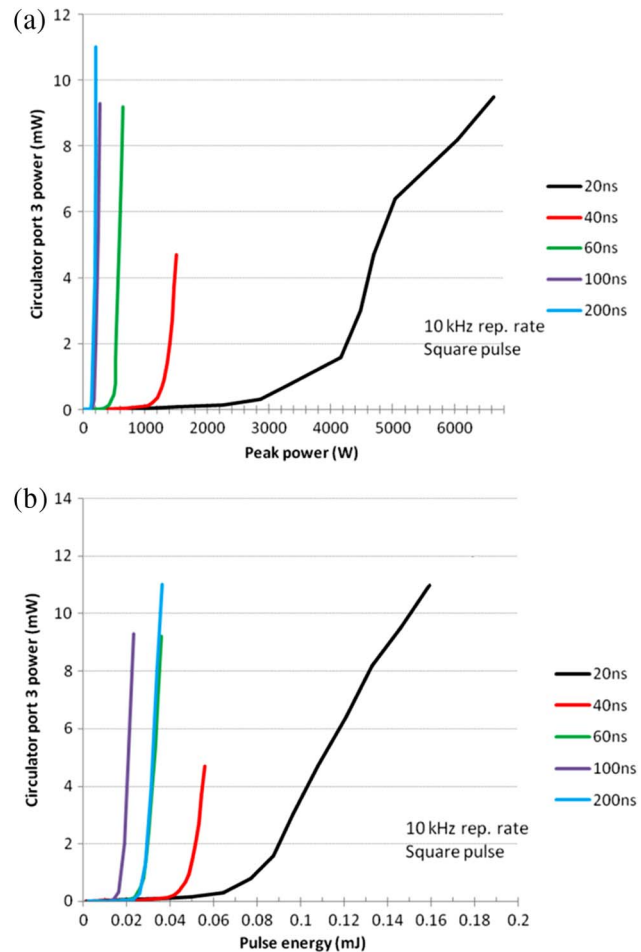

Fig. 3. (Color online) SBS power (from Circulator Port 3) as a function of: (a) Output peak power. (b) Output pulse energy.

Fig. 4. (Color online) Examples of output pulse shape: (a) Before SBS threshold. (b) After SBS threshold.

Assuming the FWHM Brillouin linewidth $\Delta\nu_{\mathrm{SBS}} = 13$ MHz at 1.5 μm [13], then the dephasing time, $T_2 \approx 20$ ns, can be calculated from the equation

$$T_2 = 1/(\pi\Delta\nu_{\mathrm{SBS}}). \qquad (2)$$

T_2 describes the required time to phase the created phonons, which establishes the macroscopic acoustic wave in the material. For pulse widths less than T_2, the SBS gain is significantly reduced.

As SBS occurs in the backward direction in fiber, the circulator's port 3 (monitor ④) was used to detect SBS signal. A trace from an optical spectrum analyzer (OSA) is given in Fig. 2. A generated SBS peak can be clearly seen and has a frequency shift of ~0.08 nm.

The SBS power at circulator port 3 was also monitored. Seed laser was operated at 10 kHz repetition rate and square shaped pulses were generated. The pulsed width (FWHM) varies from 20 ns to 200 ns. Since SBS gain is proportional to laser's intensity, we present in Fig. 3(a) the SBS power as a function of output peak power. The SBS power as a function of output pulse energy is also plotted as a reference in Fig. 3(b). After a threshold in output peak power, exponential growth in SBS power was observed as the peak power increased. The SBS threshold increased when pulse widths became shorter. When the pulse width was 20 ns, which was close to the dephasing time T_2, SBS effect was significantly suppressed.

Figure 3 shows a threshold for exponential growth in the backward SBS generation. Meanwhile in
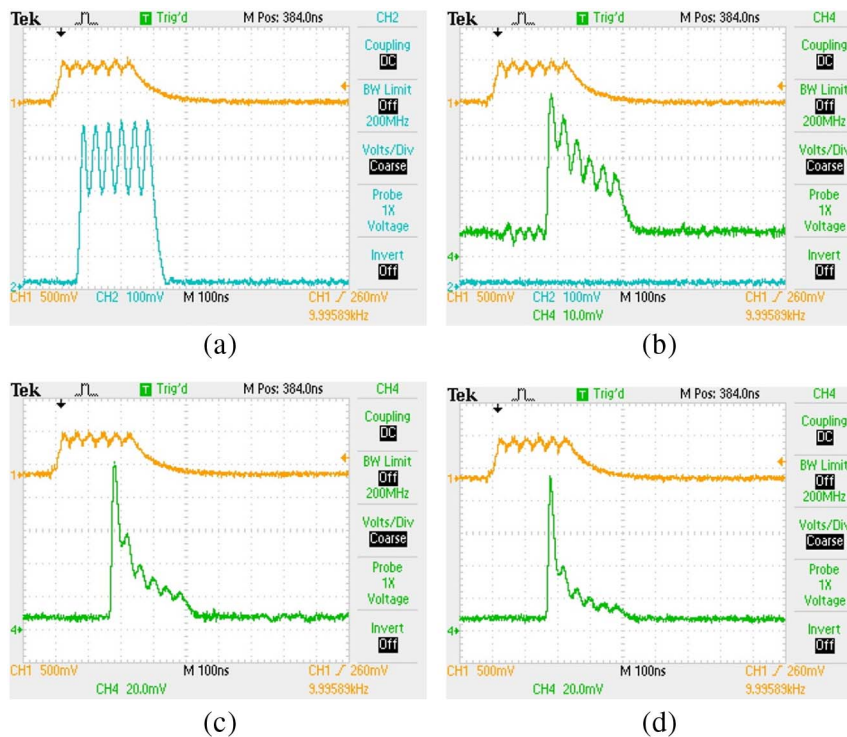

Fig. 5. (Color online) Pulse evolution at different pump current. The upper trace represents the trigger signal and the lower trace represents the laser signal. (a) 200 ns seed. (b) Output at 1.3 W pump power, pulse width was reduced to 150 ns. (c) Output at 6.6 W pump power, pulse width was reduced to 50 ns. (d) Output at 11.3 W pump power, pulse width was reduced to 15 ns.
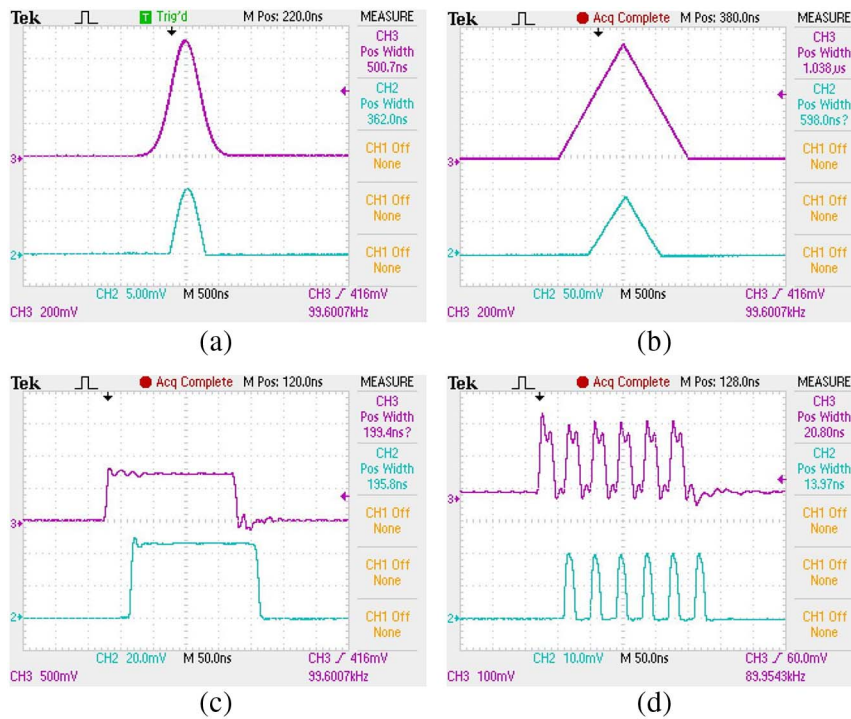
Fig. 6. (Color online) Trigger signals (upper trace) and modulated seed laser signals (lower trace) for (a) Gaussian shape, (b) triangle shape, (c) square shape, (d) a series of six individual peaks.

the forward direction, an output distortion due to transient SBS has been observed. A subpulse was added on the output main pulse when SBS threshold was reached. An example is shown in Fig. 4. Figure 4(a) is the output pulse shape before the SBS threshold. The pulse shape was stable and smooth. Figure 4(b) is the output pulse shape when strong backward SBS was detected. A depression appears in the middle of the shape, and the output pulse train was also unstable.

The SBS generation not only limits the maximum power output, it is also a threat to the laser system. Strong backward SBS generation can damage the seed laser, pumps, and other fiber components it passes through; therefore it is very important to suppress the SBS generation. From Fig. 3, a small SBS

threshold for 200 ns pulses was observed, and the output pulse energy was limited to 0.03 mJ to prevent possible SBS damaging.

Another important phenomenon observed from the experiment was that the pulse shape was significantly compressed when it evolved through the final power amplification stage. A 200 ns pulse width was compressed down to 10 ns at the highest energy level. This is partially due to the gain dynamics and partially due to the soliton formation in the anomalous dispersion fiber. Figure 5 shows the 200 ns pulse evolution at different pump levels. When the seed macropulse width was 200 ns, the output pulse width was reduced to 150 ns, 50 ns, and 15 ns at 1.3 W, 6.6 W, and 11.3 W pump power levels respectively.
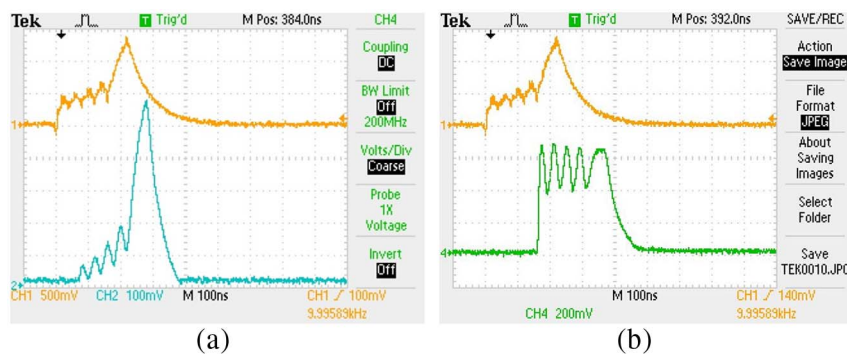

Fig. 7. (Color online) Manipulating seed pulse shape to generate ~200 ns amplified pulses. The upper trace represents the trigger signal and the lower trace represents the laser signal. (a) Seed shape. (b) At maximum pump power (13.6 W), ~200 ns macropulse width was obtained.
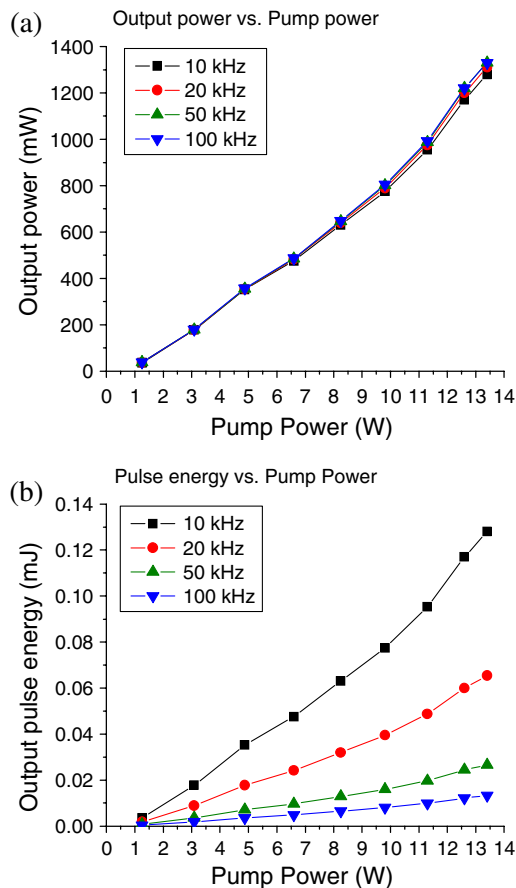
Fig. 8. (Color online) (a) Output power as a function of pump power. (b) Output pulse energy as a function of pump power.

4. Pulse Shaping Technique to Mitigate SBS and Pulse Narrowing Effects

We have successfully developed the driver board for driving a laser diode at 1.5 μm to achieve any wave format and pulse width for pulse generation. Examples of Gaussian-, triangle-, and square-shaped pulse generation are shown in Fig. 6(a)–(c), respectively. The upper trace represents the trigger signal from driving board (monitor ①) and the lower trace represents the converted optical signal from seed laser
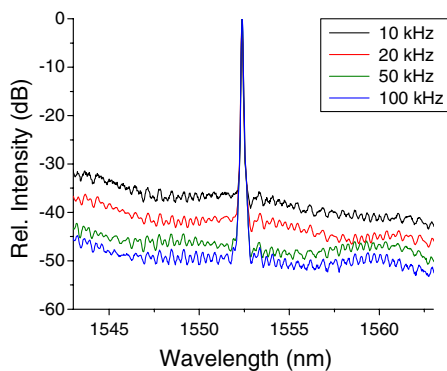

Fig. 9. (Color online) Spectra of 10 kHz, 20 kHz, 50 kHz, and 100 kHz repetition rates at maximum pump power of 13.4 W.
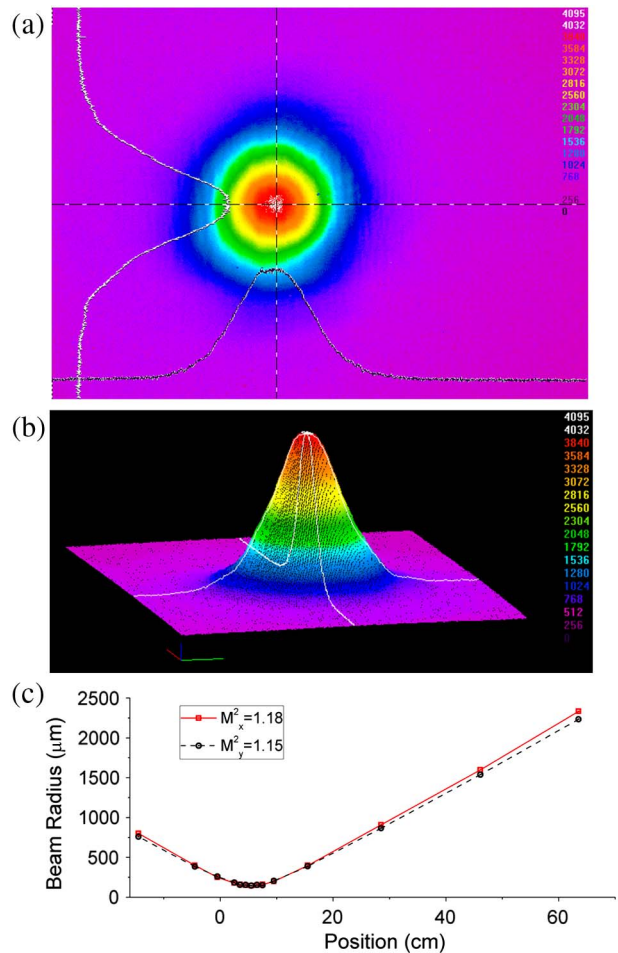
Fig. 10. (Color online) (a) and (b) The images of output pulse profile displayed in 2D and 3D views for 0.13 mJ pulses. (c) Beam quality factor M^2 measurements by scanning the beam size along the propagation direction.

(monitor ②). We were able to generate more complicated pulse shapes and one example is shown in Fig. 6(d). Within the period of 210 ns, six individual pulses were generated with only 14 ns pulse width (FWHM) each.

By manipulating a pulse shape launched into the amplifier as shown in Fig. 7, both SBS effect and pulse narrowing effect were suppressed. There are two types of modulations. One modulation is to split the 200 ns pulse into five micropulses with much narrower pulse width each. The SBS can be effectively suppressed during power amplification, because each micropulse has a shorter pulse width that increases the SBS threshold dramatically. The other modulation is to manipulate the amplitude of the micropulses. Because the leading micropulses involved higher amplification than the trailing micropulses, we generated micropulses with increasing amplitudes [Fig. 7(a)] to compensate for the pulse narrowing effect. Figure 7(b) shows the output after amplifying to the highest energy level. A 200 ns output pulse was obtained with all five micropulses at the same amplitude.

6. Characterization of 200 ns Output Pulses

We generated 200 ns pulses output at various pump power levels and repetition rates. The pump power was tuned up to 13.4 W and the repetition rate varied from 10 kHz to 100 kHz. Because of pulse narrowing effect during power amplification, we manipulated seed pulse shape under every condition to maintain the square shape and ~200 ns width for output pulses. Output power and spectra was measured during experiment. The output power as a function of pump power is plotted in Fig. 8(a) and the output pulse energy as a function of pump power is plotted in Fig. 8(b). The output powers were almost the same at different repetition rates ranging from 10 kHz to 100 kHz. The power was linear increased with pump power. The optical efficiency for the power amplifier was approximate 10%. Higher pulse energy was obtained at lower repetition rate. The maximum of 0.13 mJ was obtained at 10 kHz repetition rate and 13.4 W pump power.

The output spectrum at maximum pump power is shown in Fig. 9. The optical signal-to-noise ratio (OSNR) decreased with reduced repetition rates. Greater than 30 dB OSNR was obtained for pump power up to 13.4 W, implying the amplified spontaneous emission was effectively suppressed.

The output beam quality of the fiber laser pulse with 0.13 mJ pulse energy was characterized by a Spiricon beam profiler. Figure 10(a) and 10(b) show the images of the beam profile displayed in 2D and 3D views, which indicate the pulse has near-diffraction-limit beam quality. Beam quality factor M^2 for both horizontal and vertical directions was measured by scanning the beam size along the propagation direction, as shown in Fig. 10(c). $M^2 < 1.2$ were obtained in both directions.

7. Summary

In summary, we demonstrated a pulse shaping technology for an Er:Yb codoped fiber MOPA system at 1.5 μm to generate pulse shapes in any format. By applying such a technique, a 200 ns seed macropulse with micropulses was generated in which the SBS effect was significantly reduced, thus increasing the output power limit dramatically. We also resolved the effect of pulse narrowing during power amplification by manipulating the seed pulse shape. After power amplification, an average power of over 1.3 W and pulse energy of over 0.13 mJ were obtained at the wavelength of 1.5 μm from a gain fiber with core diameter of 17 μm. This method should be applied to other fiber laser and amplifier systems to increase the SBS threshold, thus to achieve higher energy output.

References

1. H. Hemmati, M. Wright, and C. Esproles, "High efficiency pulsed laser transmitters for deep space communications," SPIE Reviews **3932**, 188–195 (2000).
2. A. Biswas, H. Hemmati, and J. R. Lesh, "High data rate laser transmission for free space laser communications," SPIE Reviews **3615**, 269–277 (1999).
3. R. W. Ziolkowski and J. B. Judkins, "Propagation characteristics of ultrawide bandwidth pulsed Gaussian beams," J. Opt. Soc. Am. A **9**, 2021–2030 (1992).
4. D. Kelly, C. Y. Young, and L. C. Andrews, "Temporal broadening of ultrashort space-time Gaussian pulses with applications in laser satellite communication," SPIE Rev. **3266**, 231–240 (1998).
5. J. B. Hartlay, "NASA's future active remote sensing missions for earth science," SPIE Reviews **4153**, 5–12 (2001).
6. S. W. Henderson, "Eye safe coherent laser radar for range and micro Doppler measurement," Proc. IRIS Active Systems, Vol. **1**, (1997).
7. J. B. Abshire, G. J. Collatz, X. Sun, H. RiRis, A. E. Andrews, and M. Krainak, "Laser sounder technique for remotely measuring atmospheric CO2 concentrations," EOS Trans. Am. Geophys. Union **82** (2010).
8. W. Shi, E. B. Petersen, Z. Yao, D. T. Nguyen, J. Zong, M. A. Stephen, A. Chavez-Pirson, and N. Peyghambarian, "Killowatt-level stimulated-Brillouin-scattering-threshold monolithic transform-limited 100 ns pulsed fiber laser at 1530 nm," Opt. Lett. **35**, 2418–2420 (2010).
9. G. Canat, L. Lombard, S. Jetschke, S. Unger, J. Kirchhof, H. R. Müller, A. Durécu, V. Jolivet, and P. Bourdon, "Er-Yb-Doped LMA fiber structures for high energy amplification of narrow linewidth pulses at 1.5 μm," in Conference on Lasers and Electro-Optics, OSA Technical Digest Series (CD) (Optical Society of America, 2007).
10. V. Philippov, C. Codemard, Y. Jeong, C. Alegria, J. K. Sahu, J. Nilsson, and G. N. Pearson, "High-energy in-fiber pulse amplification for coherent lidar applications," Opt. Lett. **29**, 2590–2592 (2004).
11. G. P. Agrawal, *Nonlinear Fiber Optics*, 3rd ed. (Academic, 2001).
12. M. Hildebrandt, S. Buesche, P. Weβels, M. Frede, and D. Kracht, "Brillouin scattering spectra in high-power single-frequency ytterbium doped fiber amplifiers," Opt. Express **16**, 15970–15979 (2008).
13. C. E. Dilley, M. A. Stephen, and M. P. Savage-Leuchs, "High SBS-threshold, narrowband, erbium codoped with ytterbium fiber amplifier pulses frequency-doubled to 770 nm," Opt. Express **15**, 14389–14395 (2007).